### Title

Efficient Multiplexed Integration of Synergistic Alleles and Metabolic Pathways in Yeasts via CRISPR-Cas.




### Journal

Cell systems, 1(1)

### ISSN

2405-4712



### Authors

Horwitz, Andrew A
Walter, Jessica M
Schubert, Max G
et al.



### Publication Date

2015-07-01

### DOI

10.1016/j.cels.2015.02.001

Peer reviewed

Report

Cell Systems

# Efficient Multiplexed Integration of Synergistic Alleles and Metabolic Pathways in Yeasts via CRISPR-Cas

## Graphical Abstract

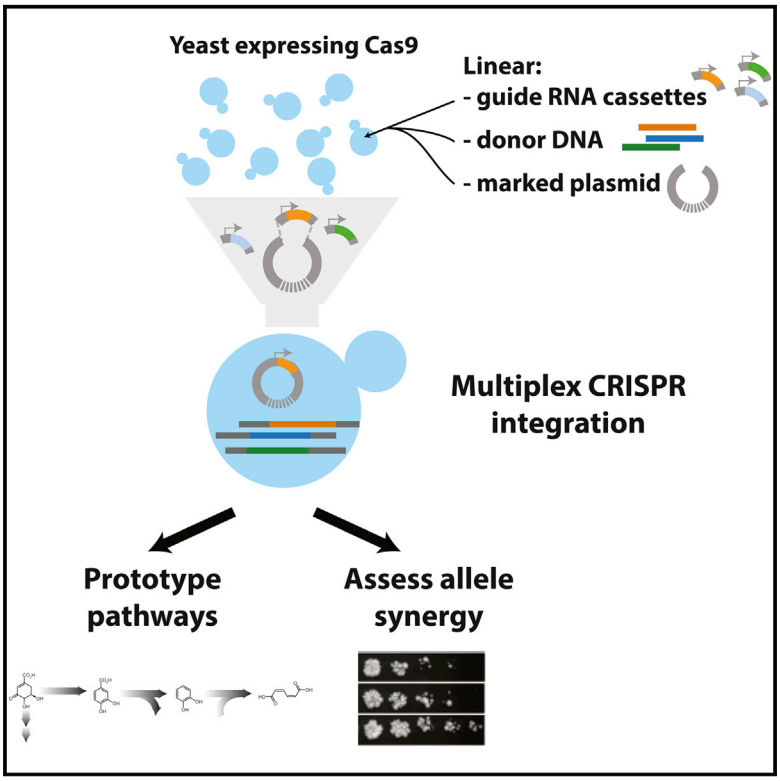


## Highlights

- A streamlined method for Cas9 guide RNA delivery speeds up genome editing in yeast
- Selection for homologous recombination competency boosts multiplex editing efficiency
- Up to five specific point mutations were introduced in one transformation
- A 24 kb/11 gene muconic acid-synthesis pathway was introduced in one transformation

## Authors

Andrew A. Horwitz, Jessica M. Walter, Max G. Schubert, ..., Wayne Szeto, Sunil S. Chandran, Jack D. Newman

## Correspondence

chandran@amyris.com

## In Brief

Horwitz et al. describe a streamlined method for using the CRISPR-Cas system in yeasts to integrate multiple DNA constructs into targeted locations in the genome with a single transformation. This method enabled rapid functional testing of combinations of mutations and prototyping of complete metabolic pathways.

Horwitz et al., 2015, Cell Systems *1*, 88–96
July 29, 2015 
http://dx.doi.org/10.1016/j.cels.2015.02.001

OPEN ACCESS
CellPress

Cell Systems
Report

# Efficient Multiplexed Integration of Synergistic Alleles and Metabolic Pathways in Yeasts via CRISPR-Cas

Andrew A. Horwitz,[1,2] Jessica M. Walter,[1,2] Max G. Schubert,[1] Stephanie H. Kung,[1] Kristy Hawkins,[1] Darren M. Platt,[1] Aaron D. Hernday,[1] Tina Mahatdejkul-Meadows,[1] Wayne Szeto,[1] Sunil S. Chandran,[1,*] and Jack D. Newman[1]
[1]Amyris, Inc., Emeryville, CA 94608, USA
[2]Co-first author
*Correspondence: chandran@amyris.com
http://dx.doi.org/10.1016/j.cels.2015.02.001


## SUMMARY

**CRISPR-Cas genome engineering in yeast has relied on preparation of complex expression plasmids for multiplexed gene knockouts and point mutations. Here we show that co-transformation of a single linearized plasmid with multiple PCR-generated guide RNA (gRNA) and donor DNA cassettes facilitates high-efficiency multiplexed integration of point mutations and large constructs. This technique allowed recovery of marker-less triple-engineering events with 64% efficiency without selection for expression of all gRNAs. The gRNA cassettes can be easily made by PCR and delivered in any combination. We employed this method to rapidly phenotype up to five specific allele combinations and identify synergistic effects. To prototype a pathway for the production of muconic acid, we integrated six DNA fragments totaling 24 kb across three loci in naive *Saccharomyces cerevisiae* in a single transformation. With minor modifications, we integrated a similar pathway in *Kluyveromyces lactis*. The flexibility afforded by combinatorial gRNA delivery dramatically accelerates complex strain engineering for basic research and industrial fermentation.**

## INTRODUCTION

Engineering microbes for industrial-scale production of materials involves iterations of a design, build, test, learn cycle. Currently, the build phase (strain engineering) is most time intensive. Top industrial production strains are heavily modified, and the use of standard methods to engineer complex pathways of this type de novo is a multi-year effort. There is an urgent need to conduct these engineering steps in parallel to speed the process. Designer nucleases can facilitate multiplex integration, and the RNA-guided CRISPR-Cas system has greatly simplified the generation of site-specific restriction endonucleases (Jinek et al., 2012). In contrast to the heterodimeric TALEN and zinc-finger nucleases, target specificity in the CRISPR-Cas system is conferred by easily programmable RNA components and can be redirected by expressing a short guide RNA (gRNA) that is complementary to the site in the genome being targeted.

As a result, there are now many reports of multiplex engineering in higher metazoans using the CRISPR-Cas system (e.g., Cong et al., 2013; Jao et al., 2013; Wang et al., 2013). Most studies use the system to induce breaks that are repaired by non-homologous end joining, leading to small deletions of variable length and loss of gene function. There are far fewer reports of integrating functional genetic constructs or introducing precise changes to genetic loci, in part owing to low rates of homologous recombination in these cell types. By contrast, *S. cerevisiae* favors homologous recombination, raising the possibility of applying the CRISPR-Cas system to more complex engineering tasks. In *S. cerevisiae*, the CRISPR-Cas system has been used to introduce a single point mutation or small construct (DiCarlo et al., 2013a), to disrupt up to three genes (Bao et al., 2014; Ryan et al., 2014), and to integrate a library of gene variants at a single locus (Ryan et al., 2014). The technique has also been adapted to fission yeast (Jacobs et al., 2014), but to our knowledge, there have been no reports of applications to other industrially relevant yeasts, such as *K. lactis*. The protocols reported to date have high efficiency but require selection for all CRISPR-Cas components, which has been achieved by cloning a complex expression plasmid for each new combination of loci targeted. This requirement limits the flexibility of these methods.

Here, we use a modular gRNA delivery strategy to achieve multiplex integration of point mutations, including simultaneous introduction of five precise modifications at three loci to confer enhanced ethanol resistance. We further apply the method for one-step integration of a muconic acid-biosynthetic pathway distributed across three loci (24 kb, 11 genes). With a slight modification of the protocol, we introduce a similar pathway design in a single transformation into a second industrially relevant yeast, *K. lactis*.

## RESULTS

### Identifying Determinants of Success for Multiplex CRISPR in *S. cerevisiae*

We set out to develop a robust method for precise, multiplex engineering via CRISPR-Cas that would enable whole-pathway

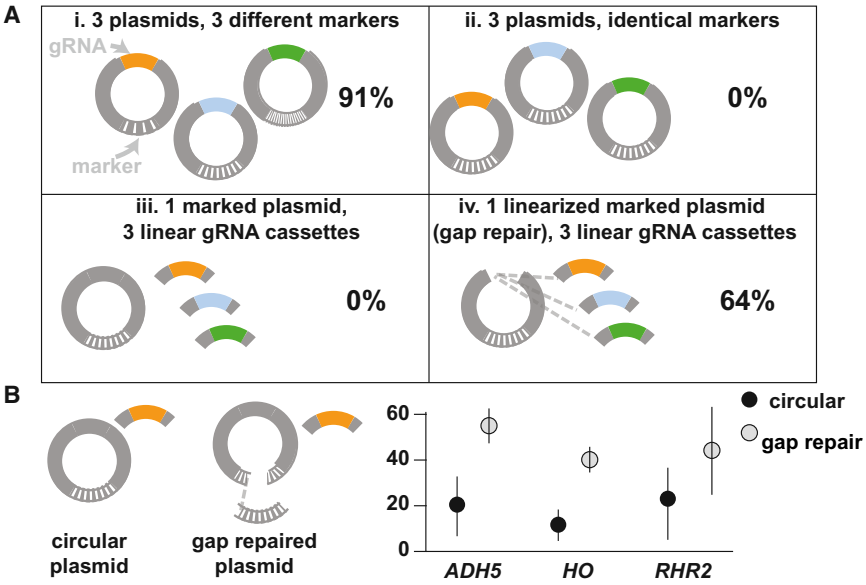


**Figure 1. A Convenient and High-Efficiency gRNA Delivery Method for Multiplex CRISPR-Cas Engineering**

(A) High rates of multiplex engineering are achievable using either multiple selection or simultaneous transformation of linear gRNA cassettes. The rate of successful triple deletion for each of four gRNA delivery methods is shown: three differently marked, circularized plasmids (91%), three circularized plasmids with the same marker (0%), one marked plasmid with three linear gRNA cassettes (0%), and one linearized marked plasmid with three linear gRNA cassettes (64%). n = 11 colonies tested per mode of gRNA delivery. (B) Requiring gap repair enhances the rate of single, marker-less integration via CRISPR-Cas. Three separate loci are shown, and each point is the average of three experiments (23 colonies assayed per experiment). By requiring repair of the marker gene on the gRNA expression plasmid, marker-less integration rates increase from 20% to 55% at *ADH5*, 12% to 41% at *HO*, and 22% to 43% at *RHR2*. Standard deviations are shown. See also Figure S1.

engineering in a single integration. Integrating a construct using the CRISPR-Cas system requires expression of Cas9p in the host cell, expression of a gRNA construct, and the provision of a donor DNA with flanking homology to the target site. We titrated Cas9p expression levels and donor DNA concentration and established that Cas9p expression level is not a sensitive parameter (Figures S1A and S1B) and donor DNA concentration is easily optimized (Figures S1C and S1D). All subsequent experiments were performed using a base strain with a Cas9 expression cassette integrated at the GRE3 locus, under control of the medium-strength FBA1 promoter. The final parameter for CRISPR-Cas genome engineering is gRNA delivery. In the original report describing a method for single-locus engineering in *S. cerevisiae*, the authors expressed the gRNA cassette from a 2μ plasmid, or from a linear cassette co-transformed with a 2μ plasmid bearing a marker for selection of transformed cells (DiCarlo et al., 2013a). The authors noted higher efficiency when the gRNA was expressed stably from a plasmid, as compared to transiently from a linear cassette. This result suggests that gRNA delivery may be a sensitive parameter. Subsequent protocols have employed a ribozyme-gRNA fusion to enhance gRNA levels (Jacobs et al., 2014; Ryan et al., 2014) and the cloning of multiple gRNA cassettes or a CRISPR RNA (crRNA) array into a single complex vector to allow selection for expression of all gRNAs or crRNAs (Bao et al., 2014; Ryan et al., 2014). To improve upon these techniques such that they might be used for routine engineering, we sought to develop a highly efficient, rapid, and cloning-free method for the combinatorial delivery of gRNAs.

## gRNA Delivery Is a Critical Parameter for Multiplexing in *S. cerevisiae*

We initially assessed four modes of gRNA delivery for simultaneous integration of a short linker sequence at the *RHR2*, *ADH5*, and *HO* loci in the *S. cerevisiae* strain CEN.PK2-1C (van Dijken et al., 2000) (Figure 1). For all modes of delivery, gRNA expression cassettes included the SNR52 promoter, the gRNA sequence, and the SUP4 terminator (DiCarlo et al., 2013a). First (mode i), gRNAs targeting each open reading frame (ORF) were cloned into separate, distinctly marked 2μ plasmids (bearing either a Ura3, His3, or nourseothricin resistance cassette), allowing for recovery of clones stably expressing all three gRNAs. Second (mode ii), the gRNAs were cloned into three plasmids bearing the same marker. Third (mode iii), the gRNA cassettes were provided as linear PCR fragments co-transformed with a 2μ plasmid bearing a nourseothricin resistance cassette. Fourth (mode iv), the gRNA cassettes were supplied as linear PCR fragments with ~500 bp of flanking homology to the ends of a linearized nourseothricin-marked 2μ plasmid to promote reconstitution of a circular plasmid in vivo by homologous recombination (gap repair) (Orr-Weaver et al., 1983). The colonies resulting from co-transformation of marker-less donor DNA and the three gRNAs were assessed by PCR (Figures 1A and S1E).

Selection for all three marked gRNA plasmids (mode i) resulted in high rates of triple integration (91%, Figures 1A and S1E). When the gRNA plasmids bore identical markers (mode ii), we observed high rates of single-locus integration but no triple-locus integrations, suggesting that explicit selection for each gRNA cassette is required. Accordingly, mode iii, without selection for any of the linear gRNA cassettes, also failed to yield triple integrations. By contrast, high rates of triple integration (64%) were observed with mode iv of gRNA delivery—namely, three linear gRNA cassettes and a single linearized 2μ plasmid bearing a marker. This result was unexpected because there is no explicit selection for stable expression of all three gRNAs. Indeed, recombination of all three gRNA cassettes into linearized 2μ plasmids in the same cell would recapitulate mode ii, which failed to yield triple integrants. Transient expression of gRNA from the cassettes is also unlikely to explain this result, as mode iii was shown to be ineffective.

### Requirement for Gap Repair Enhances Rates of Marker-less Integration by CRISPR

To investigate mechanisms underlying the efficacy of our delivery mode iv, we designed an experiment to uncouple gRNA expression from the gap repair event required for cells to attain resistance to antibiotic selection. A single, linear gRNA cassette was co-transformed with a 2μ plasmid supplied as two linear pieces: a large piece lacking only the central portion of the marker ORF and a smaller piece containing the remainder of the marker with ~125 bp flanking homology to the ORF (Figure 1B). As a control, the linear gRNA cassette was co-transformed with an intact, marked plasmid. In this experiment, the gRNA can only be expressed transiently from the linear DNA fragment, whereas selection is dependent on an intact marker plasmid. Rates of single, marker-less integration at the *RHR2*, *ADH5*, or *HO* loci were assessed in three separate experiments (Figures S1F and S1G). At each locus assayed, delivering a vector that required gap repair for marker expression increased integration rates 2- to 3-fold as compared with delivery of the intact vector (Figure 1B). As the gRNA cassette was introduced identically in both cases, this result is consistent with a hypothesis that our method enhances rates of CRISPR-Cas engineering in *S. cerevisiae* by selecting cells more capable of gap repair.

### Use of CRISPR for Introduction of Single and Multiplex Point Mutations

Next, we tested the optimized multiplex protocol (gRNA delivery mode iv) for introducing precise point mutations in *S. cerevisiae*. Introduction of a point mutation at even a single locus in *S. cerevisiae* is a tedious process. The Delitto Perfetto method allows marker-less introduction of point mutations but requires prior integration of a marked cassette containing an inducible meganuclease in close proximity to the targeted site (Moqtaderi and Geisberg, 2013). Alternatively, a marked integration cassette can be cloned (Toulmay and Schneiter, 2006). Both of these methods are problematic for essential genes, require at least two rounds of genetic engineering, and are not amenable to multiplexing. Finally, although MAGE (multiplex automated genome engineering) is an excellent option for multiplex introduction of point mutations in *E. coli*, the yeast equivalent (YOGE) functions at a much lower efficiency (Wang et al., 2009; DiCarlo et al., 2013b).

There are several considerations for the introduction of a point mutation using CRISPR-Cas. First, in addition to being unique in the genome, the site targeted for cutting should be as close as possible to the site of the desired mutation (Figure 2A). Second, the donor DNA should be designed so as to disrupt the Cas9p target site. Indeed, collateral damage to the donor DNA was cited previously to explain low rates of mutation introduction by CRISPR-Cas (DiCarlo et al., 2013a). To disrupt the Cas9p target site in the donor DNA and simultaneously improve the chances that recombination events include the desired mutation, we made silent changes in the codons between the target site and the point mutation (a "heterology block," Figure 2A). Integration of the heterology block also provides a novel primer-binding site to identify candidate clones by PCR. Because manual design of these reagents is quite time consuming, we developed an algorithm to select target sites, design gRNA cassettes, and generate donor DNA sequences with heterology blocks (unpublished data). All donor DNA constructs included ~500 bp of flanking homology.

We introduced 11 different mutant alleles into naive *S. cerevisiae* strains and tested the resulting strains for relevant phenotypes. We examined one allele relevant to industrial fermentation, conferring faster sedimentation (*ACE2* S372*) (Oud et al., 2013), a series of temperature-sensitive alleles in genes essential for cell division and the secretory pathway (*SEC1* G443E, *SEC6* L633P, *MYO2* E511K, and *CDC28* R283Q) (Lörincz and Reed, 1986; Roumanie et al., 2005), and another pair related to improved high temperature growth (*NCS2* H71L and *END3* S258N) (Sinha et al., 2008; Yang et al., 2013). Finally we tested a series of five alleles associated with resistance to elevated ethanol concentrations (*SPT15* F177S, *SPT15* Y195H, *SPT15* K218R, *PRO1* D154N, and *PUT1* deletion) (Takagi et al., 2005; Alper et al., 2006).

We observed high rates of heterology-block integration for the introduction of most individual alleles (typically > 90%, Figures S2B–S2D and Table S1), and sequencing of PCR fragments spanning the desired mutations of selected clones confirmed these changes. Incomplete separation of cells during division caused by truncation of *ACE2* was confirmed by bright-field microscopy, with dramatic clumping of cells (Figure 2B). We assayed a randomly selected confirmed clone of each temperature-sensitive mutant at permissive and restrictive temperatures to assess their phenotypes. Temperature-sensitive alleles of *CDC28*, *MYO2*, and *SEC1* failed to grow at 37°C as expected (Figure 2C), and the *CDC28* allele strain arrested in the G1 phase of growth (Figure S2A). To demonstrate secretory defects at the restrictive temperature in the *SEC1* and *SEC6* mutants, we tagged the C terminus of exocyst complex component *SEC3* with GFP at its endogenous locus (using our CRISPR-Cas approach) to function as a reporter of secretory activity. *SEC3* is normally localized to the bud in wild-type cells, but its localization is clearly disrupted in both secretory mutants (Figure 2D).

In many cases, a phenotype results from the synergy of multiple alleles, but engineering such strains is even more time consuming and is often not attempted. We applied our multiplex method to this problem. Naive CENPK2 *S. cerevisiae* bears one allele for high temperature growth (*MKT1* D30G) (Yang et al., 2013), and we introduced two additional mutations in *NCS2* and *END3*. We observed that 1/11 clones (9%) was positive for both alleles (Figure S2C; Table S1). When grown overnight at a range of temperatures, neither of the individual alleles had an effect. However, the clone containing both additional alleles integrated in a single step survived temperatures up to 42.7°C (Figure 2E).

Ethanol resistance alleles also conferred a synergistic effect. Wild-type CENPK2 tolerated up to 17.5% ethanol in our experiment (Figure 2F). Mutations in *SPT15* increased resistance up to 20% ethanol (Figure 2F). To examine the interaction of these alleles, we simultaneously introduced combinations of up to five targeted changes over three loci into a naive strain (three mutations in *SPT15*, *PRO1* D154N, and the deletion of *PUT1*). The three mutations in *SPT15* were introduced on a single donor DNA by using two gRNAs to excise ~150 bp of the gene containing the three alleles. Twenty-seven percent of the resulting clones contained all five modifications as assessed by colony PCR and confirmed by sequencing (Figure S2D; Table S1). The

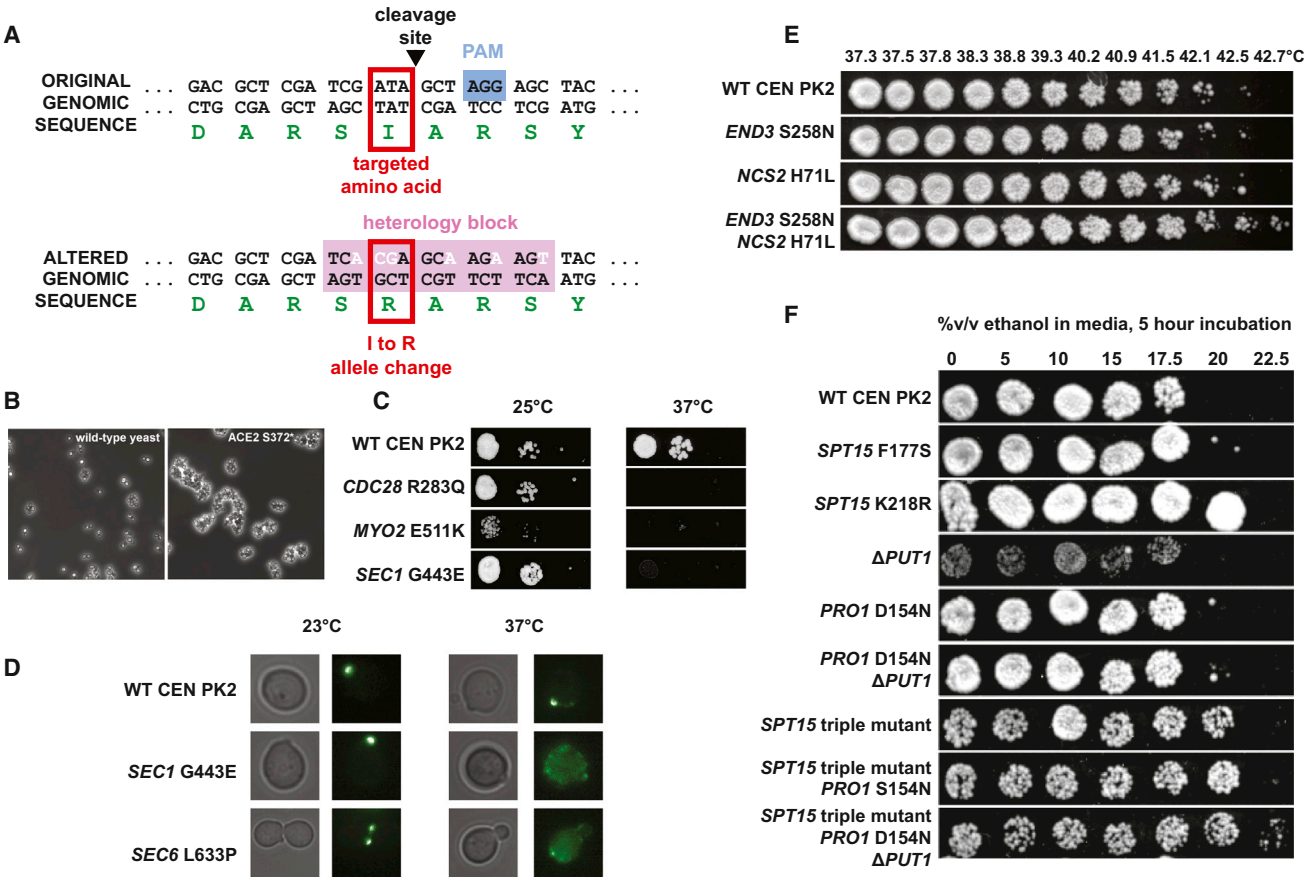


**Figure 2. Multiplexed Point Mutations Achieved with CRISPR-Cas Genome Editing Display Synergistic Phenotypes**

(A) Design of double-stranded DNA (dsDNA) donor constructs for targeted single amino-acid point mutations introduces silent amino-acid substitutions in a heterology block surrounding the point mutation and eliminates the PAM sequence.

(B) Truncation of *ACE2* results in incomplete cell division and clumping.

(C) Temperature-sensitive secretory and cell-cycle mutants of essential proteins for cell division (*CDC28*, *MYO2*, and *SEC1*) grow at the permissive temperature (25°C) but do not grow at the restrictive temperature of 37°C.

(D) *SEC3*-GFP is localized correctly to the bud at the permissive temperature (23°C) but mis-localized at the elevated temperature in strains with temperature-sensitive mutants of secretory proteins (*SEC1* G443E and *SEC6* L633P).

(E) *END3* S258N and *NCS2* H71L alleles do not individually increase heat tolerance in CEN.PK2, but when introduced in combination by CRISPR-Cas, cells are able to survive 28 hr at 42.7°C.

(F) Mutations in *SPT15* and *PRO1* individually impart some ethanol resistance in complete synthetic media containing 2% glucose. When these four alleles are introduced in combination with deletion of *PUT1* by multiplex CRISPR, ethanol tolerance is extended up to 22.5% v/v for 5 hr of exposure at 30°C.

positive clone tested had the highest ethanol tolerance, up to 22.5% (Figure 2F). It is worth noting that although rates of multiplex allele integration varied across targets and their combinations (Table S1), in all cases, we were able to recover at least one suitable clone by screening 11 colonies. As these results demonstrate, multiplexed CRISPR-Cas engineering allows rapid evaluation of hypotheses about combinations of causal alleles.

## Multiplex Integration of a Complete Muconic Acid-Biosynthetic Pathway via CRISPR-Cas

Engineering novel metabolic pathways, even in tractable hosts, is a lengthy process of sequential gene-cassette integration and marker removal. This makes rapid prototyping of novel pathways impossible, forcing engineers to commit to a particular product and pathway design from the outset. Multiplex and marker-less engineering would greatly speed this process. We attempted multiplex integration of a 24 kb pathway encoding a route to muconic acid in CENPK2 *S. cerevisiae* (Figure 3A). Muconic acid is a precursor molecule with potential for the production of bioplastics, including nylon-6,6, polyurethane, and polyethylene terephthalate (PET). Currently, muconic acid is obtained from petroleum-derived feedstocks via organic synthesis, but a renewable source is desirable for environmental reasons (Thiemens and Trogler, 1991).

Biosynthesis of muconic acid is achieved by overexpression of the aromatic amino acid (shikimate) biosynthetic pathway, and high-level production (36.8 g/l, fed batch fermentation) was achieved in *E. coli* (Niu et al., 2002). Lower pH fermentation with *S. cerevisiae* would facilitate downstream processing and industrialization of the process. There are two published reports

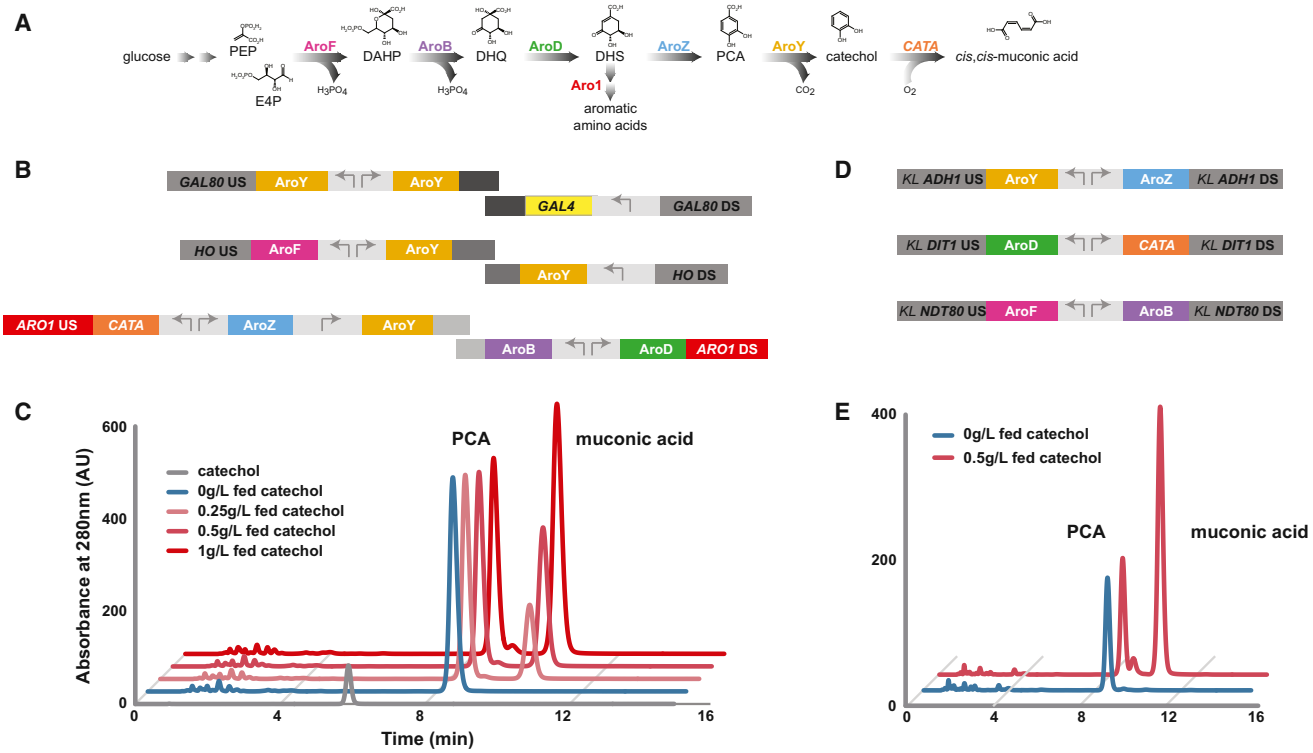


**Figure 3. The Entire Muconic Acid-Biosynthesis Pathway Can Be Integrated into Naive Yeast Strains in a Single Transformation**

(A) Schematic of the muconic biosynthesis pathway.

(B) The muconic acid pathway (11 genes distributed over 6 DNA fragments, totaling 24 kb) was introduced into three separate loci in CENPK2 *S. cerevisiae* by multiplex CRISPR-Cas engineering.

(C) Rapid confirmation of shikimate pathway functionality and identification of a pathway defect at AroY in the CENPK2 strain. Strains with the integrated pathway produce 2.7 g/l protocatechuic acid (PCA, blue). When fed catechol (gray), these strains convert all available catechol to muconic acid (red).

(D) A smaller muconic acid pathway (six genes distributed over three DNA fragments, totaling 9.7 kb) was introduced into three separate loci in *K. lactis* in a single step.

(E) *K. lactis* strains with the integrated pathway produce 0.9 g/l PCA (blue), exhibiting the same pathway bottleneck as *S. cerevisiae* strains. When fed catechol, these strains also fully convert all available catechol to muconic acid (red).

of muconic acid production in *S. cerevisiae* (Weber et al., 2012; Curran et al., 2013), and titers up to 141 mg/l have been observed in shake-flask experiments in an engineered *S. cerevisiae* strain (Curran et al., 2013). To enhance flux, we tested the *E. coli* shikimate pathway genes AroF, AroB, and AroD to replace three functions of the native pentafunctional *ARO1* gene. To troubleshoot a PCA decarboxylase bottleneck observed in two previous reports (Weber et al., 2012; Curran et al., 2013), we tested an *AroY* gene from *Acetobacter tropicalis* and incorporated five copies into our design in an attempt to achieve a high dosage (previously [Curran et al., 2013], an *E. cloacae* PCA decarboxylase was expressed from a high-copy plasmid as well as from Ty2 retrotransposon δ elements). Finally, based on the results from Curran et al., we used the *CATA* gene from *Candida albicans* to accomplish the final conversion of catechol to *cis-cis* muconic acid (Curran et al., 2013).

To test this prototype pathway, we designed six large DNA constructs bearing 11 genes to integrate over the *GAL80*, *HO*, and *ARO1* loci in CENPK2 (Figure 3B). *HO* was chosen as a neutral locus, whereas *GAL80* was selected to remove glucose repression of the galactose operon. The galactose operon was further de-repressed though expression of a copy of *GAL4* under control of a constitutive variant of the *GAL4* promoter (Griggs and Johnston, 1991). The *ARO1* locus was deleted to force flux through the engineered pathway. *ARO1* deletion also makes the strains auxotrophic for aromatic amino acids, creating a simple switch mechanism between the biomass building phase (in rich media) and the production phase (in minimal media). Complete descriptions of the pathway constructs and gene origins are provided in Table S2 and Supplemental Experimental Procedures.

We applied our optimized method for simultaneous, markerless integration of all 6 constructs, assayed 48 clones by PCR, and identified 2 clones (4.2%) that contained a triple integration event (Figure S3A). It is notable that integration of these six constructs requires nine recombination events (two flanking and one internal event per locus). Although the observed rate is lower than seen for multiplex deletions, introduction of a complete biosynthetic pathway is expected to confer a fitness defect, and we speculate that this may limit recovery of properly integrated strains.

Production of muconic acid and intermediates was tested in a 96-well shake-plate assay, with analysis by high-pressure liquid chromatography (HPLC). The one-step integrated strains showed high titers of protocatechuic acid (PCA, 2.7 g/l), indicating a non-functional AroY, the enzyme that converts PCA to catechol (Figure 3A). For comparison, these PCA titers are nearly an order of magnitude higher than previously observed in *S. cerevisiae*, confirming the high performance of the heterologous *E. coli* shikimate pathway (Curran et al., 2013). To test the functionality of the pathway downstream of PCA, we supplied up to 1 g/l catechol directly to the production media wells and observed quantitative conversion to *cis-trans* muconic acid in the engineered but not parent strain, suggesting that a single defect exists in the pathway at AroY (Figure 3C).

To test the efficacy of our method in a second industrially relevant yeast, we integrated a more compact version of the muconic acid pathway comprising six genes (9.7 kb exogenous DNA) in *K. lactis*. The pathway was divided into three integration constructs targeting the *DIT1*, *ADH1*, and *NDT80* loci (gene names are reported as *S. cerevisiae* homologs; Figure 3D and Supplemental Experimental Procedures). A naive *K. lactis* strain (ATCC 8585) was prepared by integrating Cas9 at the *GAL80* locus and deleting *YKU80* to minimize the effects of non-homologous end joining (Kooistra et al., 2004; Wésolowski-Louvel, 2011). Marker-less integration of all three constructs was accomplished in one step using our method, with the modification that the linearized plasmid contained the pKD1 stability element (Chen et al., 1988). To our knowledge, no other group has reported the use of the CRISPR-Cas system in *K. lactis*. Triple integrations occurred at a rate of 2.1%, as assayed by PCR (n = 48, Figure S3B). Similar to the results in *S. cerevisiae*, we observed high titers of PCA (0.9 g/l) but no muconic acid production (Figure 3E). Catechol feeding experiments confirmed the same defect in AroY function (Figure 3E). It is notable that we did not delete *ARO1* in our *K. lactis* strain, and this discrepancy may explain the lower titers of PCA we observed. In summary, in less than 1 month, we were able to prototype a pathway for muconic acid production in two industrially relevant yeast strains and thus establish a workflow that facilitates rapid design iterations and host flexibility.

## DISCUSSION

The optimized CRISPR-Cas-based engineering method presented here greatly compresses the timeline for engineering biosynthetic pathways in yeast, and its specificity is determined by modular PCR-generated gRNA cassettes. We and others have observed that gRNA expression is a key variable for multiplexing in *S. cerevisiae* at high efficiency (Figure 1) (Ryan et al., 2014). Although we found the p*SNR52* gRNA cassette reported previously to be sufficient in *S. cerevisiae* (DiCarlo et al., 2013a), Ryan et al. and Jacobs et al. enhanced gRNA levels by fusion to a ribozyme (Jacobs et al., 2014; Ryan et al., 2014) and addressed multiplexing by sub-cloning multiple gRNA cassettes into a single vector (Ryan et al., 2014). Likewise, Bao et al. cloned all components (including small donor DNAs) into a single vector prior to using the CRISPR-Cas system (Bao et al., 2014). Through selection for the plasmid, these protocols ensure sustained expression of all RNA components, similar to the selection scheme we described in Figure 1 (mode i). Ryan et al. were able to achieve rates of triple gene disruption of ~80% using flanking homology regions of just 50 bp (Ryan et al., 2014). Bao et al. achieved rates of 27%–87%, or up to 100% with multiple day outgrowth in liquid media, using similarly short flanking homology regions (Bao et al., 2014).

Our method relieves the requirement for coordinated selection of all gRNAs, while maintaining high rates of multiplexed engineering. For triple gene deletions, we report a rate of 64%, in line with the efficiencies reported by Ryan et al. and Bao et al. and sufficient to recover desired clones with minimal screening. It is fair to note that our homology flanks are longer than those used in the previous reports (500 bp versus 50 bp). However, for routine use, our method of gRNA delivery offers considerable logistical advantages. The previously described methods involve restriction cloning of large plasmids bearing repetitive sequences, requiring multiple days to prepare and validate, whereas the gRNA reagents for our method can be generated by PCR on the same day as transformation and delivered in any combination desired without additional preparation.

The efficacy of this mode of gRNA delivery is notable, as there is no sustained selection for expression of all gRNA cassettes. Our results indicate that delivery of linear constructs requiring gap repair into a linearized plasmid can enhance rates of marker-less integration at genomic sites (Figure 1B). Examination of gRNA-containing plasmids from yeast colonies resulting from successful editing of three loci using our method (Figure 1B) revealed that only one of the three gRNA species is represented per colony assayed (six plasmid clones were sequenced from eight different yeast colonies; data not shown). Although it is possible that multiple gap-repaired species co-exist at earlier time points (prior to colony formation), this result suggests that gap repair is not primarily involved in gRNA expression kinetics. Rather, we propose that gap repair identifies a special subpopulation of transformed cells. Competency for homologous recombination is known to vary throughout the cell cycle (Symington and Gautier, 2011), and the asynchronous mixture of log-phase cells used for transformation would be expected to contain cells in all states. Indeed, rates of homologous recombination can be improved by chemically synchronizing cells in late G2 or S phase of the cell cycle (Saleh-Gohari and Helleday, 2004; Lin et al., 2014). If yeast cells most proficient in gap repair are also best equipped to accomplish multiplex integrations, then this capability may allow marker-less, multiplex integrations to proceed with only transient expression of the gRNAs. Nevertheless, further work will be required to confirm these hypotheses. Regardless of precise mechanism, there may be opportunities to combine our method with some of the innovations reported by Bao et al. (2014), Jacobs et al. (2014), and Ryan et al. (2014). For example, fusion of a ribozyme to the gRNA construct might further improve efficiencies of the method reported here by enhancing gRNA levels in the cell.

The time savings realized through multiplexed engineering are substantial. The introduction of three point mutations in an *S. cerevisiae* strain requires approximately 6 weeks with standard methods (1 week to introduce each allele, 1 week to recycle each marker, 3 cycles total), compared to just 1 week when using multiplexed CRISPR-Cas. This efficiency permits rapid testing of ambitious hypotheses. For example, we revealed the synergy

of four point mutations and a deletion to increase ethanol tolerance in CENPK2 *S. cerevisiae* in a single round of engineering (Figure 2F). The timeline for prototyping a large muconic acid pathway at three loci was likewise compressed 6-fold. We rapidly confirmed the efficacy of the heterologous shikimate pathway in *S. cerevisiae* and identified a pathway defect (AroY). The gains in efficiency of multiplex engineering scale with the number of loci targeted, and the maximum number of loci that can be targeted simultaneously is unclear, although we have engineered up to five loci simultaneously in our work with production strains at Amyris (data not shown). By reducing the time commitment required to realize individual strain designs, multiplex CRISPR-Cas genome editing will allow strain engineers to pursue more hypotheses and more rapidly identify high-flux biosynthetic pathways for use at the industrial scale.

## EXPERIMENTAL PROCEDURES

### Preparation of *S. cerevisiae* and *K. lactis* Host Strains for CRISPR-Cas

CRISPR-Cas engineering requires the Cas9 protein. We designed and ordered an *S. cerevisiae* codon-optimized version of the *Streptococcus pyogenes* Cas9 gene fused to an SV40 nuclear localization sequence (DiCarlo et al., 2013a) and cloned it into an integration cassette under the expression of the strong *FBA1* promoter (or, for examination of Cas9p expression effects, a range of promoters) with a *CYC1* terminator (Supplemental Sequences). The construct, marked with an hphA (hygromycin resistance) cassette, was stably integrated at the *GRE3* locus of a naive CENPK2 strain or at the *GAL80* locus of *K. lactis* (ATCC 8585). The *YKU80* locus was subsequently deleted in this *K. lactis* strain via CRISPR to reduce rates of non-homologous end joining. Plasmids are described in Table S4.

### Selection of Target Sites

Potential Cas9p targets are canonically described by the sequence $N_{(20)}$NGG. The NGG sequence is referred to as a protospacer adjacent motif (PAM) sequence, and the 8 bp of DNA preceding the PAM sequence are especially important for enforcing specificity (Fu et al., 2013; Hsu et al., 2013). A search method was developed to (1) identify all possible CRISPR sites occurring within ORFs in the yeast genome and then (2) rank them based on several parameters. To avoid off-target cutting, our method eliminated candidate sites with high similarity to other genomic sites in the 8 bp of PAM-proximal sequence (2 bp or fewer substitutions). Additionally, sites that contain runs of five or more thymines were eliminated, as they have the potential to terminate RNA polymerase III transcripts (DiCarlo et al., 2013a).

### gRNA Expression Cassettes and Plasmids

Cas9p is targeted to cut sites by association with a generic structural RNA and a specific targeting RNA. We adopted the standard "chimeric" configuration, in which the targeting and structural RNAs are fused to create a single gRNA (Jinek et al., 2012; Cho et al., 2013; Ran et al., 2013). Expression of the gRNA construct was driven by the *SNR52* polymerase III promoter, with a *SUP4* terminator (DiCarlo et al., 2013a). The gRNA cassette was cloned into pRS4XX-series 2μ vectors (Sikorski and Hieter, 1989), either (1) by standard cloning methods to generate finished plasmids prior to transformation into a Cas9-expressing yeast strain, (2) by gap repair directly into a Cas9-expressing host strain (Orr-Weaver et al., 1983), or (3) by co-transformation of the linear cassette with a closed plasmid bearing a selectable marker. For transformations into *K. lactis*, we modified the *S. cerevisiae* 2μ plasmid to include a stabilizing pKD1 element (Chen et al., 1988). To create circular plasmids, we co-transformed annealed oligonucleotides containing the CRISPR target sequence and 20 bp of upstream/downstream homology to the cassette with a linearized backbone in *E. coli* (Mandecki, 1986), identified correct clones, and then transformed the plasmid into a host strain. To gap repair the gRNA cassette directly into the 2μ vector in the host strain, we first generated full-length gRNA cassettes with ~500 bp flanking homology to the linearized vector. Using a generic gRNA cassette as template, we amplified half cassettes using primers to create a central overlap of 19 bp containing the unique CRISPR target sequence. The two half cassettes were then assembled in a second PCR reaction to generate a full-length gRNA expression cassette. We used 10 μl of unpurified PCR assembly (typically 20–60 ng/μl concentration as determined by comparison to DNA marker ladder), or multiple assemblies for multiplex attempts, and 100–150 ng of linearized 2μ vector per transformation. Plasmid, gRNA, and primer sequences are supplied in Tables S3 and S4.

### Preparation of Donor DNA for Integrations and Deletions

Donor DNA constructs with ~500 bp of flanking homology (or ~1,000 bp for the *K. lactis* constructs) were generated by our in-house automated strain engineering (ASE) service using standardized linkers for assembly. For deletions, a linker was the only intervening sequence and served as a primer site for colony PCR reaction to confirm the genomic deletion event. 400–1,000 ng of donor DNA were used in each transformation. Sequences and primers are provided in Table S3.

### Integration of Marker-less DNA

To test whether CRISPR enables marker-less integration at a single locus, we used optimized LiAc methods to co-transform donor DNA and the appropriate gRNA reagents into each Cas9-expressing strain (Gietz and Woods, 2002). Cells were grown overnight in yeast extract peptone dextrose (YPD) media at 30°C with shaking, then diluted to an optical density (OD) 600 of 0.175 in flasks and grown again at 30°C with shaking to $OD_{600}$ 0.7. Cells were spun down, resuspended in sterile water, spun down, resuspended in 100 mM lithium acetate, spun down, and resuspended in 100 mM lithium acetate (50 μl per transformation). Transformation mix included the following: 240 μl 50% PEG 3350, 36 μl 1M lithium acetate, 10 μl boiled salmon sperm DNA (10 mg/ml), and 74 μl DNA and cells. Cells were recovered overnight in non-selective YPD media before plating to selective, antibiotic-containing media to maintain the gRNA plasmid (usually nourseothricin). Marker-less integrations were scored as positive if colony PCR yielded amplicons at the 5′ and/or 3′ integration flanks, a result indicative of a targeted integration event.

### Determination of Optimal Donor DNA Concentration

To optimize donor DNA concentrations, we investigated deletion of the *RHR2* locus using the protocols described here (gRNA delivery mode i) and donor DNA concentrations ranging from 1 to 100 fmol of donor DNA. Rates of *RHR2* deletion were assessed by the described colony PCR protocol, and colonies were counted on fractional platings of transformation mixture to assess the relationship between addition of donor DNA and cell survival.

### Use of CRISPR-Cas for Introducing Point Mutations

The selection of Cas9p target sites for introducing point mutations is considerably more constrained than for deletion or integration into an ORF. We developed an algorithm to identify the most suitable sites and generate gRNA and donor DNA designs (unpublished data). Donor DNAs were designed with ~500 bp of flanking homology surrounding a central "heterology block." The heterology block introduces silent mutations to the sequence surrounding the Cas9p target site and serves several purposes. First, it removes bases critical for CRISPR-Cas recognition, such that the donor DNA will not be cut. Second, it is designed to reduce homology to the target sequence and accordingly increase the probability that the desired mutation will be incorporated during repair of the double-stranded break. Third, the heterology block introduces a unique sequence that can be used as a primer site for preliminary confirmation of clones by PCR. See Table S3 for a full description of these reagents.

### Integration of Marker-less Point Mutations

The transformation procedure for point mutations is identical to the standard protocol, with an additional step required to confirm clones. Initial candidates were identified by colony PCR using a primer inside the introduced heterology block and an outside, flanking primer. The point-mutation region was then amplified from re-streaked candidates and sequenced to confirm the change at single bp resolution. Temperature-sensitive mutants were incubated at 25°C instead of 30°C.

### Assay for Temperature Sensitivity

A randomly selected clone from sequence-confirmed secretory mutants and wild-type CENPK2 was grown at 25°C overnight and then diluted into two identical tubes of complete synthetic media (CSM) 2% glucose. One tube was incubated with shaking at 25°C and one at 37°C. One hour later, cultures were compared by microscope. For growth assays, the overnight culture was spotted with 10-fold dilutions onto a YPD plate and incubated at room temperature for 3 days or at 37°C overnight.

### Assay for Heat Tolerance

Wild-type CENPK2 and a randomly selected clone from the sequence-confirmed *END3* and *NCS3* individual and combined mutants were grown overnight in liquid YPD at 30°C. Strains were diluted to $OD_{600}$ 0.05 in CSM 2% glucose and incubated in PCR tubes in a gradient PCR machine from 37.3°C to 42.7°C. Strains were spotted on YPD plates undiluted and at 1:10, 1:100, and 1:1000 dilutions at 28 hr.

### Assay for Ethanol Tolerance

A randomly selected sequence-confirmed strain was grown overnight in liquid YPD at 30°C. In the morning, cultures were diluted to $OD_{600}$ 0.1 in CSM 2% glucose in 1.1 ml polypropylene 96-well plates at a gradient of ethanol concentrations (0%, 5%, 10%, 15%, 17.5%, 20%, and 22.5% v/v). The plate was covered with an impermeable plastic seal. Strains were incubated without shaking at room temperature for 5 hr and then plated onto YPD undiluted and at 1:10 and 1:100 dilutions.

### Assays for Muconic Acid Production

Colonies of putative muconic acid production strains were picked into 96-well shake-plates and grown at 30°C in YPD media for 48 hr. Cells were spun down, and the YPD replaced with production media (4% sucrose minimal media) and grown for 72 hr. Supernatants were obtained and analyzed by HPLC using the following parameters: mobile phase—0.15% formic acid in 95:5 water:methanol, flow rate: 0.6 ml/min (isocratic), analysis time: 15.0 min, wavelength: 280 nm (214 nm for muconolactone), injection volume: 2.0 μl, column temperature: 40.0°C, column: Agilent ZORBAX Bonus-RP 5.0 μm, 3.0 × 150 mm (Product no. 883668-301). A series of pathway intermediate retention time standards were used to identify peaks from unknown samples. For catechol feeding experiments, catechol (Sigma #135011) was added at various concentrations to the production media.

## SUPPLEMENTAL INFORMATION

Supplemental Information includes Supplemental Experimental Procedures, three figures, and four tables and can be found with this article online at http://dx.doi.org/10.1016/j.cels.2015.02.001.

## AUTHOR CONTRIBUTIONS

A.A.H., J.M.W., M.G.S., S.H.K., K.H., D.M.P., A.D.H., T.M.-M., and W.S. designed and conducted experiments. A.A.H., W.S., S.S.C., and J.D.N. supervised research. A.A.H. and J.M.W. wrote the manuscript.

## ACKNOWLEDGMENTS

This work was produced with Government support under Agreement HR0011-12-3-0006, awarded by DARPA. We are grateful to Alicia Jackson and Thomas Armel of DARPA for their critical comments over the course of the project. We thank the many members of the Amyris community who supported this effort, including Joel Cherry for support and feedback on the manuscript, Stefan Moser for assistance with HPLC assays, the Automated Strain Engineering group for assembly of DNA constructs, and Lab Services for reagents, media, and strain banking. At the time this work was produced, all authors were employees and shareholders of Amyris, Inc.

Received: November 17, 2014
Revised: January 12, 2015
Accepted: February 18, 2015
Published: March 12, 2015

## REFERENCES

Alper, H., Moxley, J., Nevoigt, E., Fink, G.R., and Stephanopoulos, G. (2006). Engineering yeast transcription machinery for improved ethanol tolerance and production. Science *314*, 1565–1568.

Bao, Z., Xiao, H., Liang, J., Zhang, L., Xiong, X., Sun, N., Si, T., and Zhao, H. (2014). Homology-integrated CRISPR-Cas (HI-CRISPR) system for one-step multigene disruption in Saccharomyces cerevisiae. ACS Synth Biol. http://dx.doi.org/10.1021/sb500255k.

Chen, X.J., Wésolowski-Louvel, M., Tanguy-Rougeau, C., Bianchi, M.M., Fabiani, L., Saliola, M., Falcone, C., Frontali, L., and Fukuhara, H. (1988). A gene-cloning system for Kluyveromyces lactis and isolation of a chromosomal gene required for killer toxin production. J. Basic Microbiol. *28*, 211–220.

Cho, S.W., Kim, S., Kim, J.M., and Kim, J.S. (2013). Targeted genome engineering in human cells with the Cas9 RNA-guided endonuclease. Nat. Biotechnol. *31*, 230–232.

Cong, L., Ran, F.A., Cox, D., Lin, S., Barretto, R., Habib, N., Hsu, P.D., Wu, X., Jiang, W., Marraffini, L.A., and Zhang, F. (2013). Multiplex genome engineering using CRISPR/Cas systems. Science *339*, 819–823.

Curran, K.A., Leavitt, J.M., Karim, A.S., and Alper, H.S. (2013). Metabolic engineering of muconic acid production in Saccharomyces cerevisiae. Metab. Eng. *15*, 55–66.

DiCarlo, J.E., Norville, J.E., Mali, P., Rios, X., Aach, J., and Church, G.M. (2013a). Genome engineering in Saccharomyces cerevisiae using CRISPR-Cas systems. Nucleic Acids Res. *41*, 4336–4343.

DiCarlo, J.E., Conley, A.J., Penttilä, M., Jäntti, J., Wang, H.H., and Church, G.M. (2013b). Yeast oligo-mediated genome engineering (YOGE). ACS Synth Biol *2*, 741–749.

Fu, Y., Foden, J.A., Khayter, C., Maeder, M.L., Reyon, D., Joung, J.K., and Sander, J.D. (2013). High-frequency off-target mutagenesis induced by CRISPR-Cas nucleases in human cells. Nat. Biotechnol. *31*, 822–826.

Gietz, R.D., and Woods, R.A. (2002). Transformation of yeast by lithium acetate/single-stranded carrier DNA/polyethylene glycol method. Methods Enzymol. *350*, 87–96.

Griggs, D.W., and Johnston, M. (1991). Regulated expression of the GAL4 activator gene in yeast provides a sensitive genetic switch for glucose repression. Proc. Natl. Acad. Sci. USA *88*, 8597–8601.

Hsu, P.D., Scott, D.A., Weinstein, J.A., Ran, F.A., Konermann, S., Agarwala, V., Li, Y., Fine, E.J., Wu, X., Shalem, O., et al. (2013). DNA targeting specificity of RNA-guided Cas9 nucleases. Nat. Biotechnol. *31*, 827–832.

Jacobs, J.Z., Ciccaglione, K.M., Tournier, V., and Zaratiegui, M. (2014). Implementation of the CRISPR-Cas9 system in fission yeast. Nat. Commun. *5*, 5344.

Jao, L.E., Wente, S.R., and Chen, W. (2013). Efficient multiplex biallelic zebrafish genome editing using a CRISPR nuclease system. Proc. Natl. Acad. Sci. USA *110*, 13904–13909.

Jinek, M., Chylinski, K., Fonfara, I., Hauer, M., Doudna, J.A., and Charpentier, E. (2012). A programmable dual-RNA-guided DNA endonuclease in adaptive bacterial immunity. Science *337*, 816–821.

Kooistra, R., Hooykaas, P.J., and Steensma, H.Y. (2004). Efficient gene targeting in Kluyveromyces lactis. Yeast *21*, 781–792.

Lin, S., Staahl, B.T., Alla, R.K., and Doudna, J.A. (2014). Enhanced homology-directed human genome engineering by controlled timing of CRISPR/Cas9 delivery. Elife *3*, e04766, http://dx.doi.org/10.7554/eLife.04766.

Lörincz, A.T., and Reed, S.I. (1986). Sequence analysis of temperature-sensitive mutations in the Saccharomyces cerevisiae gene CDC28. Mol. Cell. Biol. *6*, 4099–4103.

Mandecki, W. (1986). Oligonucleotide-directed double-strand break repair in plasmids of Escherichia coli: a method for site-specific mutagenesis. Proc. Natl. Acad. Sci. USA *83*, 7177–7181.

Moqtaderi, Z., and Geisberg, J.V. (2013). Construction of mutant alleles in Saccharomyces cerevisiae without cloning: overview and the delitto perfetto method. Curr. Protoc. Mol. Biol. *104*, 10C.

Niu, W., Draths, K.M., and Frost, J.W. (2002). Benzene-free synthesis of adipic acid. Biotechnol. Prog. *18*, 201–211.

Orr-Weaver, T.L., Szostak, J.W., and Rothstein, R.J. (1983). Genetic applications of yeast transformation with linear and gapped plasmids. Methods Enzymol. *101*, 228–245.

Oud, B., Guadalupe-Medina, V., Nijkamp, J.F., de Ridder, D., Pronk, J.T., van Maris, A.J., and Daran, J.M. (2013). Genome duplication and mutations in ACE2 cause multicellular, fast-sedimenting phenotypes in evolved Saccharomyces cerevisiae. Proc. Natl. Acad. Sci. USA *110*, E4223–E4231.

Ran, F.A., Hsu, P.D., Wright, J., Agarwala, V., Scott, D.A., and Zhang, F. (2013). Genome engineering using the CRISPR-Cas9 system. Nat. Protoc. *8*, 2281–2308.

Roumanie, O., Wu, H., Molk, J.N., Rossi, G., Bloom, K., and Brennwald, P. (2005). Rho GTPase regulation of exocytosis in yeast is independent of GTP hydrolysis and polarization of the exocyst complex. J. Cell Biol. *170*, 583–594.

Ryan, O.W., Skerker, J.M., Maurer, M.J., Li, X., Tsai, J.C., Poddar, S., Lee, M.E., DeLoache, W., Dueber, J.E., Arkin, A.P., and Cate, J.H. (2014). Selection of chromosomal DNA libraries using a multiplex CRISPR system. Elife *3*, http://dx.doi.org/10.7554/eLife.03703.

Saleh-Gohari, N., and Helleday, T. (2004). Conservative homologous recombination preferentially repairs DNA double-strand breaks in the S phase of the cell cycle in human cells. Nucleic Acids Res. *32*, 3683–3688.

Sikorski, R.S., and Hieter, P. (1989). A system of shuttle vectors and yeast host strains designed for efficient manipulation of DNA in Saccharomyces cerevisiae. Genetics *122*, 19–27.

Sinha, H., David, L., Pascon, R.C., Clauder-Münster, S., Krishnakumar, S., Nguyen, M., Shi, G., Dean, J., Davis, R.W., Oefner, P.J., et al. (2008). Sequential elimination of major-effect contributors identifies additional quantitative trait loci conditioning high-temperature growth in yeast. Genetics *180*, 1661–1670.

Symington, L.S., and Gautier, J. (2011). Double-strand break end resection and repair pathway choice. Annu. Rev. Genet. *45*, 247–271.

Takagi, H., Takaoka, M., Kawaguchi, A., and Kubo, Y. (2005). Effect of L-proline on sake brewing and ethanol stress in Saccharomyces cerevisiae. Appl. Environ. Microbiol. *71*, 8656–8662.

Thiemens, M.H., and Trogler, W.C. (1991). Nylon production: an unknown source of atmospheric nitrous oxide. Science *251*, 932–934.

Toulmay, A., and Schneiter, R. (2006). A two-step method for the introduction of single or multiple defined point mutations into the genome of Saccharomyces cerevisiae. Yeast *23*, 825–831.

van Dijken, J.P., Bauer, J., Brambilla, L., Duboc, P., Francois, J.M., Gancedo, C., Giuseppin, M.L., Heijnen, J.J., Hoare, M., Lange, H.C., et al. (2000). An interlaboratory comparison of physiological and genetic properties of four Saccharomyces cerevisiae strains. Enzyme Microb. Technol. *26*, 706–714.

Wang, H., Yang, H., Shivalila, C.S., Dawlaty, M.M., Cheng, A.W., Zhang, F., and Jaenisch, R. (2013). One-step generation of mice carrying mutations in multiple genes by CRISPR/Cas-mediated genome engineering. Cell *153*, 910–918.

Wang, H.H., Isaacs, F.J., Carr, P.A., Sun, Z.Z., Xu, G., Forest, C.R., and Church, G.M. (2009). Programming cells by multiplex genome engineering and accelerated evolution. Nature *460*, 894–898.

Weber, C., Brückner, C., Weinreb, S., Lehr, C., Essl, C., and Boles, E. (2012). Biosynthesis of cis,cis-muconic acid and its aromatic precursors, catechol and protocatechuic acid, from renewable feedstocks by Saccharomyces cerevisiae. Appl. Environ. Microbiol. *78*, 8421–8430.

Wésolowski-Louvel, M. (2011). An efficient method to optimize Kluyveromyces lactis gene targeting. FEMS Yeast Res. *11*, 509–513.

Yang, Y., Foulquié-Moreno, M.R., Clement, L., Erdei, E., Tanghe, A., Schaerlaekens, K., Dumortier, F., and Thevelein, J.M. (2013). QTL analysis of high thermotolerance with superior and downgraded parental yeast strains reveals new minor QTLs and converges on novel causative alleles involved in RNA processing. PLoS Genet. *9*, e1003693.